Molecular Crystals and Liquid Crystals Science and Technology. Section A. Molecular Crystals and Liquid Crystals

Publication details, including instructions for authors and subscription information:
http://www.tandfonline.com/loi/gmcl19

The Characteristics of SSFLC Cells with Stripe-Shaped Domain Structure

Ruibo Lu [a], Keshu Xu [a], Shuyan Zhang [a], Yongkang Le [a], Huihua Deng [b], Ning Gu [b] & Zuhong Lu [b]

[a] Department of Physics, State Joint Key Laboratory for Materials Modification by Laser, Ion and Electron Beams, Fudan University, Shanghai, 200433, China

[b] National Laboratory of Molecular and Biomolecular Electronics, Southeast University, Nanjing, 210018, China

Version of record first published: 24 Sep 2006

To cite this article: Ruibo Lu, Keshu Xu, Shuyan Zhang, Yongkang Le, Huihua Deng, Ning Gu & Zuhong Lu (1999): The Characteristics of SSFLC Cells with Stripe-Shaped Domain Structure, Molecular Crystals and Liquid Crystals Science and Technology. Section A. Molecular Crystals and Liquid Crystals, 333:1, 35-45

To link to this article: http://dx.doi.org/10.1080/10587259908025994

Mol. Cryst. Liq. Cryst., Vol. 333, pp. 35-45
Reprints available directly from the publisher
Photocopying permitted by license only

The Characteristics of SSFLC Cells with Stripe-Shaped Domain Structure

RUIBO LU[a*], KESHU XU[a], SHUYAN ZHANG[a], YONGKANG LE[a], HUIHUA DENG[b], NING GU[b] and ZUHONG LU[b]

[a]Department of Physics, State Joint Key Laboratory for Materials Modification by Laser, Ion and Electron Beams, Fudan University, Shanghai 200433, China and [b]National Laboratory of Molecular and Biomolecular Electronics, Southeast University, Nanjing 210018, China

(Received 20 January, 1998; In final form 29 October, 1998)

The stripe-shaped domain (SSD) structure has been obtained in the initial ferroelectric liquid crystal (FLC) alignment by doping phthalocyanine compound into the rubbed polyimide films. Atomic force microscopy (AFM) was used to investigate the aligning films and the corresponding aligning ability was evaluated through the pre-tilt angle measurement. The memory capability and the contrast ratio of the aligned SSFLC cells have been enhanced and improved with the appearance of the SSD structure. In addition, the stability of 64 × 80 electrically controlled FLC spatial light modulator has been improved, too. The possible formation mechanism of the SSD structure was also discussed.

Keywords: ferroelectric liquid crystal; stripe-shaped domain; atomic force microscopy; alignment; spatial light modulator

1. INTRODUCTION

It has been two decades passed since the first synthesis of ferroelectric liquid crystal (FLC) compound[1,2] and the later invention of surface-stabilized ferroelectric liquid crystal (SSFLC) mode[3], which has attracted great research enthusiasm for its high content, fast response time and memory capability, while it seems that there still has a quite long way to go before the commercialization of SSFLC devices. The appearance of zig-zag defects and the stability of the SSFLC cells are two major serious obstacles that hinder the SSFLC devices to be commercialized because the existence of the zig-zag defects can deteriorate the electro-optic properties of the cells and the shock-sensitive FLC alignment, the

* Correspondence Author.

degeneracy of the aligned SmC* layer structure after a certain period of operation et al. are not expected for the application aim. Although a tristable ferroelectric / antiferroelectric material has been synthesized[4] and some kinds of novel effects, such as distorted helical ferroelectric (DHF) effect[5], short-pitch bistable ferroelectric (SBF) effect[6] and twisted SmC*effect[7], have been proposed, it is still interesting to explore SSFLC devices for its quick response and optical bistability to allow large multiplexing rates, especially compared with NLC devices.

Some methods have been used for the elimination of zig-zag defects in SSFLC cells. From the view of near-surface alignment, special polyimide (PI) films[8] and glancing-angle evaporated SiO films[9], which provide a high pre-tilt angle to FLC molecules, can ensure a unidirection-bent SmC* layer and avoid the cusping of the neighboring layers with contrary senses to form a zig-zag defect line. AC stabilization has also been proved effective to get rid of zig-zag defects under the application of a strong electric field[10,11]. An alternative way to overcome this problem, rather than the use of special surface alignments or treatment with large electric fields, is the use of alternative FLC materials. The FLC mixtures containing materials derived from napthalene rings could produce bookshelf-type structure when cooled from SmA phase to SmC* phase and defect-free alignment can be obtained[12]. Antiferroelectric liquid crystal mixtures are another type candidate materials, where self-recovery of the smectic layer can occur even if it is damaged[13].

As a special case of the zig-zag defects, the stripe-shape domain (SSD) structure can be got when an external electric field was applied in the SmA or SmC* phase during the temperature lowering process of the cells[14–16]. The SSD structure can maintain a good memory capability and has the possibility to be more stable for its peculiar configuration compared with the other type of alignment textures existed in SSFLC cells.

In this paper, we adopted a rubbed and doped PI films instead of the reported PVA to align FLC and obtained a uniform SSD structure in the initial alignment, which can still be kept under the AC application. The e-o properties of the aligned SSFLC cells have been measured at different rubbing strength. A 64×80 electrically controlled, matrix-addressed FLC spatial light modulator (SLM) was fabricated using the new aligning films to get a SSD structure. The characteristics of the device was also investigated. The formation mechanism of the SSD was discussed from the physical-chemical interaction view through AFM observations and pre-tilt angle measurement.

2. EXPERIMENTAL

Tin phthalocyanine, which is abbreviated as SnPc. was doped into a silicon-contained polyamic acid at the doping ratio ranging from 0.5:1 to 2:1 in mole. The

solution was spun onto the ITO substrates at the spinning speed of 3,500 revolutions per minute. The substrates were imidized at the temperature of 200°C for 2 hours. The resulted PI films were uniformly rubbed under a moving, velvet-coated cylinder and a SSFLC cell was fabricated with the rubbing direction parallel to each other. The cell thickness was controlled at 1.5~1.8 μm.

FLC SCE-13 (BDH Co., British) was injected into the cell by the capillary action when heated high above the clearing point, then slowly cooled down to the room temperature at the rate of 0.3 °C/min. The FLC material has a phase sequence of Crystal –20°C SmC^* 60.8°C SmA 86.3°C N^* 100.8°C Isotropic.

An antiparallel type cell was assembled for the measurement of pre-tilt angle in the nematic phase, where the crystal rotation method was used at the measurement precision up to 0.01° (DMS-501, Germany). The cell thickness was controlled at 50 μm. NLC ZLI-3417–006 (E. Merck Darmstadt) was poured into the cell under a vacuum condition.

The e-o properties of the SSFLC cells were measured by placing them between crossed polarizers. The light transmission signals were probed and recorded by a photomultiplier and a dual-trace memory oscilloscope. The contrast ratio (Cr) between the bright state and the dark state was obtained by rotating the cell surface perpendicular to the incident light at the maximum value when no voltage was applied, or measured under the application of a ± 20 v, 10 Hz square voltage pulses. The rising time is defined as the time when the transmission intensity attains from 10% to 90%, while the decaying time is calculated when the transmission intensity lowers from 90% to 10%. The memory ratio (Mr) was measured under a 1 ms bipolar pulse with a period of 20 ms and defined as $Mr = \frac{M_L + M_D}{2}[\%]$, where M_L and M_D are the contrast ratios in the bright and dark states respectively, as in reference 17.

AFM (Nanoscope III, Digital Instrument Inc., USA) observations were carried out on the ITO substrates directly under a constant force mode in the air condition of 20°C. The force between the AFM tip and the substrate was of the order of 10 nN.

3. RESULTS AND DISCUSSION

3.1 Polarized microscope observation

Figure 1 are the typical SSD structures of the SSFLC cells observed under the polarized microscope near the extinction position, which surfaces were rubbed

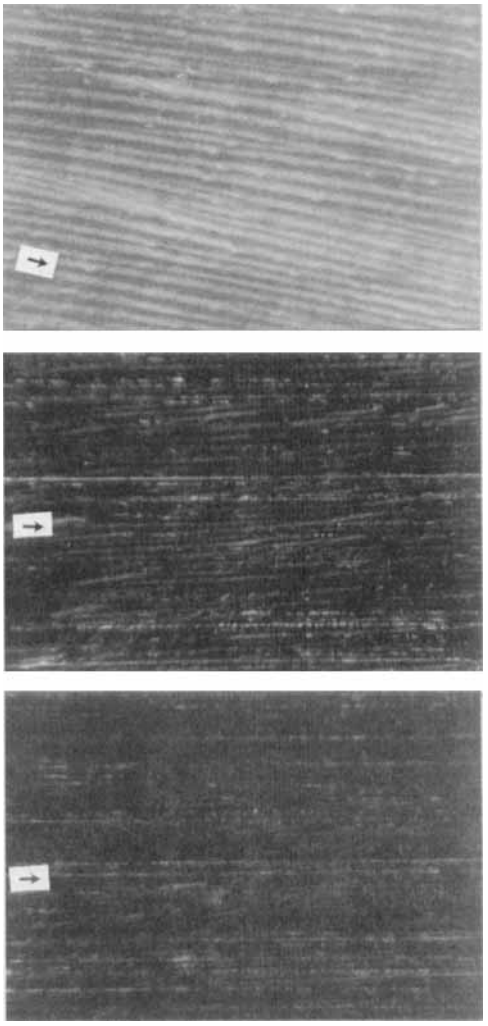

FIGURE 1 The SSD structure in SnPc doped SSFLC cells observed under the polarized microscope, where (a), (b) and (c) correspond to the cells aligned by the films rubbed at weak, medium and strong strengths, respectively. The arrow indicates the film rubbing direction (See Color Plate I at the back of this issue)

by weak, medium and strong rubbing strengths respectively at the dopant ratio of 0.5:1. The SSD structures are long and narrow with the average widths of 11 μm, 7 μm and 3 μm corresponding to the weak, medium and strong rubbing strengths, which are mainly aligned along the surface-rubbed directions. The SSD structures can be retained when observed under the microscope during the cooling, re-heating and then cooling process. It reveals that the FLC molecules

are divided into many separate domain regions and are liable to be aligned uniaxially by the rubbing process due to the strong surface anchoring ability that can be attributed to the surface memory effect.

In a 64 × 80 pixel FLC SLM, obvious SSD structure can also be observed in individual pixels as shown in Figure 2. The average width of the SSD is about 7 μm. The thinner width is beneficial to get a high information content for a transmissive type SLM.

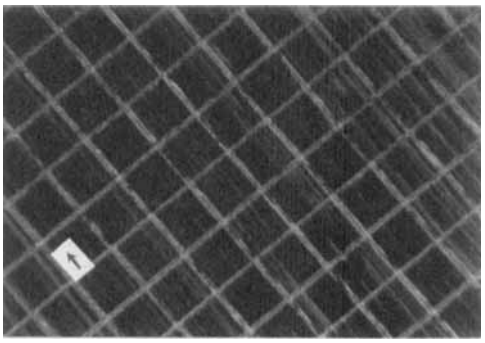

FIGURE 2 The SSD structure in 64 × 80 FLC SLM observed under the polarized microscope. The arrow indicates the film rubbing direction (See Color Plate II at the back of this issue)

3.2 AFM images

Figure 3 are AFM images of doped aligning films rubbed under different rubbing strengths. The films were all uniformly rubbed after the unidirectional rubbing and formed a groove structure, where the protruding aggregate polymer chains are orderly oriented along the rubbing direction. The strong strength rubbed films have denser and thinner grooves compared with the medium and weak rubbed ones at an average groove width of 18 nm. The strong strength rubbed films have also a higher depth at about 1 nm. The weakly rubbed film has a less ordered polymer chain orientation after the mechanical rubbing.

It has been found that the appearance and formation of the SSD structure is concerned of the dopant ratio, the rubbing force and the FLC material adopted, while the width of the SSD is directly connected with the rubbing strength applied on the aligning films. To a SSFLC cell with a thickness of 1.5 μm, the width will decrease with the increase of rubbing strength in a certain range and the cell has a higher SSD structure density. At the strong rubbing strength, the SSD structure is thinner and more discernible than that of the weakly rubbed cell when observed near the extinction position under the polarized microscope.

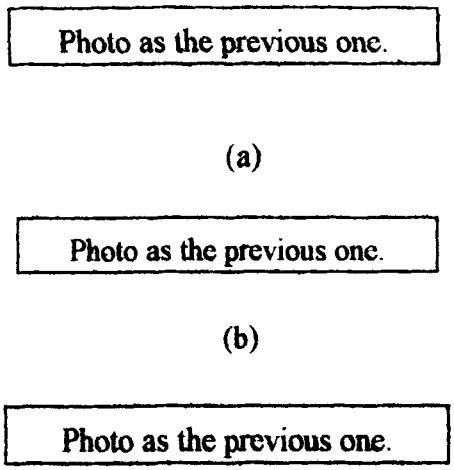

FIGURE 3 AFM images of SnPc doped aligning films under different rubbing strength. The images (a), (b) and (c) correspond to the films rubbed at strong, medium and weak strengths, respectively

Since the stronger rubbing strength produces a denser SSD structure, it can be seen that the rubbing formed grooves are main factors that determine the density of the SSD. The topology of the nano-scaled polymer films may play an important role in the LC alignment and have a certain effect on the formation of the SSD structure.

3.3 Pre-tilt angle measurement at different dopant ratio

The measured pre-tilt angles of NLC on the medium strength rubbed PI films at different dopant ratios are shown in Figure 4. Although there has no obvious relationship between the pre-tilt angle and the dopant ratio, which may be incurred by the doping process that complexes the inner actions in the Pc-PI system and thus influences the interfacial interactions between LC and the aligning layers, it can still be certain that a relative low pre-tilt angle is beneficial to the formation of the SSD structure. On the other hand it has also found that there has no much variation in the pre-tilt angle under different rubbing strengths in our investigated range.

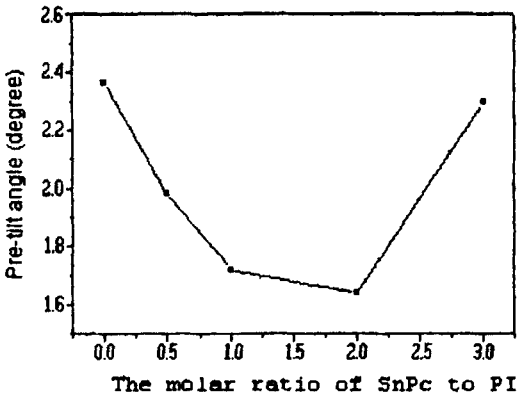

FIGURE 4 The relationship between the pre-tilt angle of NLC and the molar ratio of SnPc to PI

3.4 E-o characteristics of SSD cells

The contrast ratio and memory capability of the SSD cells treated under different rubbing strength were investigated and listed in Table I.

It is interesting to notice that after the doping process, the memory capabilities of the SSFLC cells have improved significantly and show an excellent bistability compared with that of the non-doped one, irrespective of the rubbing strength applied.

Since the doped SnPc belongs to a kind of organic semiconductor, which has a certain conductivity, the memory capability difference can be explained by the rapid charge compensation model in the ultra-thin and conductive aligning layers, where the surface charges brought out during the switching process can be neutralized quickly after the removal of the outer voltage as in the case of LB films and TCNQ doped charge-transfer complex aligning films[18,19].

TABLE I The contrast ratio (Cr) and memory ratio (Mr) of the SSFLC SSD cells

Alignment Layer	*Rubbing Strength*	*Cr*	*Mr (%)*
Doped Cell	Strong	1.7/21	*/82
	Medium	6.3/70	*/100
	Weak	5.8/82	*/100
Non-doped Cell	Medium	4.2/35	* /40

* The doped molar ratio is 0.5:1. The upper and lower part in Cr and Mr represents the ratio without and with AC electric field application respectively. The rubbing strength is applied in a certain range at the precondition that both the strong and the weak rubbing could provide a homogeneous FLC alignment.

Under different rubbing strengths, the doped cells have an obvious variation in Cr with and without voltage application. The strong strength rubbed cell has a lowest Cr both before and under the AC application. It demonstrates that hard rubbed surface has a stronger anchoring effect and thus formed FLC defects are incurable and show no extinction position even under AC stabilization, but it can still maintain the structure irreversibility to provide the memory state[20]. To the medium and weak rubbed cells, the respective Cr under AC is much higher than that of without AC application. In addition, they all have a higher Cr than the strong rubbed cell. This may be attributed to its easy formation of a bookshelf or quasi-bookshelf structure under the electric field[16,21].

3.5 E-o characteristics of SLM

The measured response times of 64 × 80 FLC SLM are 80 μs and 75 μs to the rising and decaying period, respectively. The contrast ratio between the switched ON and OFF state is 64. Figure 5 shows the bistability of the SLM under the periodic pulse, which also has an excellent memory capability of nearly 100.

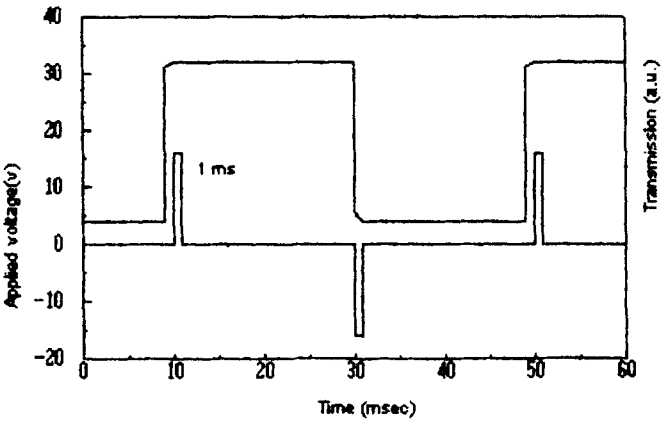

FIGURE 5 Optical response of SnPc doped rubbing films aligned 64 × 80 FLC SLM. The applied voltage is ± 16 V under a 1 ms bipolar pulse with a period of 20 ms

After the SLM has been stored and operated for more than one year, the SSD structure keeps unchanged and the e-o characteristics has no obvious degeneracy, which is different from our previous non-doped SLMs that the e-o properties would deteriorate after a certain period storage with the collapse of the aligning layer. It indicates that the SSD structure is stable and FLC SLM with this structure has an improved stability, which is valuable as a practical device.

3.6 The formation mechanism of the SSD structure

As we have observed through the AFM investigation, it reveals that there has a groovy structure at the nano-scale that is comparable to the size of FLC molecules. The orderly oriented aggregate polymer chains that are formed by the unidirectional rubbing force were also observed. The existence of the rubbed grooves can guide the LCs to align preferentially along the wavy topological surface in the isotropic and N^* phase during the initial FLC injection process. Therefore, the grooves have the ability to provide an anisotropic action on the LCs physically, especially in the nematic phase[22,23].

It has been proved that the formation of a homogeneous LC alignment requires a strong surface pinning effect from the aligning films to realize the surface-stabilized state in SmC^*. The SnPc doped cells have a lower pre-tilt angle than that of the non-doped one, which indicates that the LCs are induced heavier in the longitutial axis by the molecular interactions, such as the dispersive force, in the neighboring interface between the LCs and the aligning film, while the orderly elongated polymer chains guarantee the molecular interactions effective in a preferred direction to get a uniform LC alignment. The relative low pre-tilt angle means that LCs tend to lie on the rubbed surface by the strong anchoring force. The FLC material used in our condition has a phase sequence of K-SmC^*-SmA-N^*-I. So, in the FLC cooling process a homogenous alignment of N^* phase can be firstly obtained. Later the smectic layer is formed and perpendicular to the substrate surface through the transition to SmA. If the smectic layer is maintained after the phase transition SmA-SmC^*, the bookshelf structure can be realized. While due to the layer shrinkage in the SmA-SmC^*phase transition, to keep the density stable and energy minimized, chevron structure can be easily formed. In the interface between two neighboring chevrons with contrary senses, defect lines usually occur[24,25]. We think the appearance of the narrow and long SSD structure in our condition is from the uniform physical topology and the molecular interactions on one part. On the other part, it may be the most stable layer structure of the static equilibrium configuration, which has been proved by our device fabrication of FLC SLM.

Since the width of our SSD structure is wider than the previously reported, we propose our model is an expanded SSD structure compared with that of Y.Asao et al.[21]. Based on the fact that the width is influenced by the topology of the aligning layers and a low pre-tilt angle can not provide a unidirectional-bent SmC^* layer as the possible case of a high pre-tilt angle[8], we conjecture that, after crossing a certain number of groovy surfaces, the neighboring chevrons having several layer width will tilt in the contrary sense and meet, cusp together to form the interface that develops the SSD structure definitively. The detailed layer

structure needs an accurate probing technique, such as X-ray diffraction, and it will be carried out later.

4. CONCLUSIONS

We have obtained the uniform SSD structure in the FLC initial alignment by doping SnPc into the rubbed PI films and investigated the e-o characteristics of the corresponding SSFLC cells. The memory capability and the contrast ratio of the aligned SSFLC cells have been enhanced and improved with the appearance of the SSD structure. A similar case is also to thus fabricated FLC SLM, which shows an excellent e-o properties and improved stability. We discussed the SSD formation mechanism phenomenologically from the physical-chemical interaction view and regarded that the orderly oriented topology of the aligning layers and an appropriate anchoring ability from the interface between the LC and the rubbing films are essential for the formation of the SSD structure.

Acknowledgements

This work was financially supported by the National Educational Foundation of China.

References

[1] R.B. Meyer, L. Liebert, L. Strzelecki and P. Keller, J. Phys. Paris, **36,** L69 (1975).
[2] R.B. Meyer, Mol. Cryst. Liq. Cryst., **40,** 33 (1977).
[3] N.A. Clark and S.T. Lagerwall, Appl. Phys. Lett. **36,** 899 (1980).
[4] A.D. Chandani, E. Gorecka, Y. Ouchi, H. Takezoe and A. Fukuda, Jpn. J. Appl. Phys. **28,** 1265 (1989).
[5] L.A. Bersnev, V.G. Chigrinov, D.I. Dergachev, E.P. Poshichaev, J. Fµnfscniling and M. Schadt, Liq. Cryst. **5,** 1171 (1989).
[6] J. Fµnfscniling and M. Schadt, Jpn. J. Appl. Phys. **30,** 741 (1991).
[7] J.S. Patel, Appl. Phys. Lett. **60,** 280 (1992).
[8] N. Yamamoto, Y. Yamada, K. Mori, H. Orihara and Y. Ishibashi, Jpn. J. Appl. Phys. **28,** 524 (1989).
[9] S. Kaho, T. Masumi, S. Tahata, M. Mizunuma and S. Miyake, Jpn. J. Appl. Phys. **199,** 87 (1991).
[10] Y. Sato, T. Tanaka, H. Kobayashi, K. Aoki, H. Watanabe, H. Takeshita, Y. Ouchi, H. Takezoe and A. Fukuda, Jpn. J. Appl. Phys. **28,** L483 (1989).
[11] S.S. Bawa, K. Saxena and S. Chandra, Jpn. J. Appl. Phys. **28,** 662 (1989).
[12] Y. Takanishi, Y. Ouchi, H. Takezoe, A. Fukuda, A. Mochizuki and M. Nakatsuka, Jpn. J. Appl. Phys. **29,** 984 (1990).
[13] K. Itoh, M. Johno, Y. Takanishi, Y. Ouchi, H. Takezoe and A. Fukuda, Jpn. J. Appl. Phys. **30,** 735 (1991).
[14] L. Lejcek and S. Pirkl, Liq. Cryst. **8,** 871 (1990).
[15] J. Pavel and M. Glogarova, Liq. Cryst. **9,** 87 (1991).
[16] R.F. Shao, P.C. Willis and N.A. Clark, Ferroelectrics **121,** 127 (1991).
[17] K. Nakaya, B. Zhang, M. Yoshiba, I. Isa, S. Shindoh and S. Kobayashi, Jpn. J. Appl. Phys. **28,** L116 (1989).

[18] H. Ikino, A. Oh-Saki, M. Nitta, N. Ozaki, Y. Yokoyama, K. Nakaya and S. Kobayashi, Jpn. J. Appl. Phys. **27,** L475 (1988).
[19] K. Nakaya, B.Y. Zhang, M. Yoshida, I. Isa, S. Shindoh and S. Kobayashi, Jpn. J. Appl. Phys. **28,** L116 (1989).
[20] M. Isogai, M. Oh-e, T. Kitamura and A. Mukoh, Mol. Cryst. Liq. Cryst. **207,** 87 (1991).
[21] Y. Asao and T. Uchida, Jpn. J. Appl. Phys. **32,** L604 (1993).
[22] U. Wolf, W. Greubel and D. Kruger, Mol. Cryst. Liq. Cryst. **23,** 187 (1973).
[23] J.M. Geary, J.W. Goodby, A.R. Kmetz, and J.S. Patel, J. Appl. Phys. **62,** 4100 (1987).
[24] A. Fukuda, Y. Ouchi, H. Arai, H. Takano, K. Ishikawa and H. Takezoe, Liq. Cryst. **5,** 1055 (1989).
[25] T.P. Rieker and N.A. Clark: *Phase Transitions in Liquid Crystals* (Plenum Press, New York, 1992) Chap. 21.